JOURNAL OF AGRICULTURAL AND FOOD CHEMISTRY
ARTICLE

J. Agric. Food Chem. 2009, 57, 10341–10348 10341
DOI:10.1021/jf901608n

Synthesis and Structural Characterization of Two Diasteroisomers of Vinylcatechin Dimers

Luís Cruz,[†] Natércia F. Brás,[‡] Natércia Teixeira,[†] Ana Fernandes,[†] Nuno Mateus,[†] Maria João Ramos,[‡] José Rodríguez-Borges,[†] and Victor de Freitas*,[†]

[†]Centro de Investigação em Química and [‡]REQUIMTE, Departamento de Química, Faculdade de Ciências, Universidade do Porto, Rua do Campo Alegre, 687, 4169-007 Porto, Portugal

8-Vinylflavan-3-ols are described in the literature as the intermediate compounds involved in the formation mechanism of pyranoanthocyanins in wines or in model-like solutions. 8-Vinyl-(+)-catechin has shown to be very unstable in solution and revealed a high reactivity with itself, undergoing an unusual acid-catalyzed dimerization in model wine solution involving the formation of a new dihydropyran ring. Two diasteroisomers, (9*S*,11*R*)- and (9*R*,11*S*)-vinylcatechin dimers, were obtained, and their structures were characterized by mass spectrometry (MS) and nuclear magnetic resonance (NMR). These compounds were also found to occur in reactions between (+)-catechin and acetaldehyde. The identification of different conformations of both isomers was achieved by computational methods. The enthalpy values calculated suggest that isomer (9*S*,11*R*) is more stable and its formation is thermodynamically favored when compared to isomer (9*R*,11*S*).

KEYWORDS: (+)-Catechin; 8-vinylcatechin; dimerization; reactivity; stability; mass spectrometry; NMR

INTRODUCTION

Flavonoid compounds are present in many plants and result from their secondary metabolism. They constitute a large diversity of complex and heterogeneous chemical structures and can be found in many fruits, vegetables, and particularly, some beverages, such as tea, berry juices, and wine (*1*, *2*). Two important families present in wines are the anthocyanins and the flavan-3-ols (catechins and proanthocyanidins) that are directly related to the color and taste, respectively. Overall, these compounds possess a high reactivity, which is due to the acidic character of the phenolic groups, to the nucleophilic character of the phloroglucinol ring A and to the electrophilic character of the central pyran ring C (*3*−*5*). Therefore, during processing, storage, and wine aging, anthocyanins and flavan-3-ols may undergo several different kinds of reactions, giving rise to a large number of new and more stable products, which seem to contribute to the modification of some wine organoleptic characteristics, such as color, astringency, bitterness, and aroma (*6*−*10*). Over the last few years, several families of anthocyanin derivatives have been reported to occur in wines and wine-like solutions. Among the new pigments detected thus far, pyranoanthocyanins gained increasing attention because of the large number of compounds detected in wines and their unusual spectroscopic properties (*11*). This group of compounds include the orange color Vitisin B-type pigments (*12*), the anthocyanin−pyruvic acid adducts or Vitisins A-type pigments (orange color), resulting from reactions between anthocyanins and pyruvic acid (*12*−*15*), the red−orange pyranoanthocyanin−flavan-3-ols pigments (*16*−*19*), and the vinylpyranoanthocyanins or portisins, which present a unique bluish color (*20*−*26*). The formation of pyranoanthocyanin−flavan-3-ols in red wines is described in the literature to result from the reaction between anthocyanins and vinylflavan-3-ol adducts as intermediates (*16*). Recently, important insights concerning the formation mechanism of pyranomalvidin-3-glucoside−(+)-catechin and the involvement of vinylcatechin were provided (*27*). The formation of the intermediate vinylcatechin in wines can occur through different mechanisms, such as the dehydration of the flavanol−acetaldehyde adducts or the cleavage of ethyl-linked flavanol adducts both formed from the reaction of flavanols with acetaldehyde (*27*, *28*). Nevertheless, the occurrence of vinylcatechin adducts in wines has never been detected probably because of its great reactivity. Bearing this in mind, the present work deals with the structural characterization of 8-vinylcatechin derivatives, such as vinylcatechin dimers, obtained in model wine solutions.

MATERIALS AND METHODS

Reagents. (+)-Catechin was purchased from Sigma-Aldrich (Madrid, Spain). Acetaldehyde was obtained from Fluka Chemika (Buchs, Switzerland). TSK Toyopearl gel HW-40(S) was purchased from Tosoh (Tokyo, Japan). 8-Vinylcatechin was synthesized according to the procedures described elsewhere (*29*). The final product was a mixture of 8-vinylcatechin and (+)-catechin (1:0.3) itself, which is a byproduct formed during the Suzuki reaction by debromination of 3′,4′,5,7-tetra-*O*-*tert*-butyldimethylsilyl-8-bromocatechin. Several experiments to purify 8-vinylcatechin were performed by column chromatography techniques without any success.

Stability of 8-Vinylcatechin. A solution 8-vinylcatechin (3.2 mM) was incubated in 20% EtOH/H_2O solutions at pH 2.5, 3.5, and 4.5 and at 30 °C. The stability of 8-vinylcatechin in the three solutions was monitored over time (72 h) by high-performance liquid chromatography (HPLC) with diode array detection (DAD) at 280 nm and mass spectrometry (MS).

*To whom correspondence should be addressed. Telephone: +351-220402558. Fax: +351-220402658. E-mail: vfreitas@fc.up.pt.

Published on Web 10/09/2009

Synthesis of Vinylcatechin Dimers. A solution of 8-vinylcatechin (1.5 mM) was prepared in 20% EtOH/H_2O at pH 2 and 30 °C. The formation of the 8-vinylcatechin dimers was monitored over time by HPLC−DAD/MS at 280 nm. After 2 h, the 8-vinylcatechin dimerization reaction was stopped and the respective derivative products were purified.

Purification of Vinylcatechin Dimers. The solvent of the reactional mixture was eliminated by evaporation, and the residue was then applied onto a TSK Toyopearl gel HW-40 (S) column (250 × 16 mm inner diameter) connected to a ultraviolet (UV) detector coupled with a paper register. The flow rate was regulated at 0.8 mL/min using a peristaltic pump. The attenuation and the sheet speed were set to 256 and 0.1 cm/min, respectively. The elution was performed with methanol, and the detection wavelength was selected to 300 nm. (+)-Catechin and other impurities were collected after 1 h; vinylcatechin dimers were collected after 2 h; and vinylcatechin trimers were collected after 3 h. After removal of methanol on a rotary evaporator, the fractions containing the vinylcatechin dimers yielded an amorphous beige powder (∼20 mg), which was used for the nuclear magnetic resonance (NMR) analyses.

Reaction between (+)-Catechin and Acetaldehyde. A solution containing (+)-catechin (41 mM)/acetaldehyde (molar ratio of 1:50) was prepared in 12% EtOH/H_2O at pH 3, 4, and 6 (adjusted with acetic acid) and at 30 °C. The reaction was monitored over time by HPLC−DAD at 280 nm.

HPLC−DAD Analysis. The samples were analyzed by HPLC (Merck-Hitachi L-7100) on a 150 × 4.6 mm inner diameter, 5 μm, reversed-phase C18 column (Merck, Darmstadt, Germany) thermostatted at 25 °C; detection was carried out at 280 nm using a diode array detector (Merck-Hitachi L-7450A). Solvents were (A) a mixture of 9:1 water/formic acid (v/v) and (B) acetonitrile, with the gradient 10−35% B over 50 min at a flow rate of 0.5 mL/min. The sample injection volume was 20 μL. The chromatographic column was washed with 100% B for 10 min and then stabilized with the initial conditions for another 10 min.

LC−DAD/ESI−MS Analysis. A Finnigan Surveyor series liquid chromatograph, equipped with a Thermo Finnigan (Hypersil Gold) reversed-phase column (150 × 4.6 mm, 5 μm, C18), thermostatted at 25 °C was used. The samples were analyzed using the same solvents, gradient, injection volume, and flow rate referred above for HPLC analysis. Double-online detection was performed by a photodiode spectrophotometer and MS. The mass detector was a Finnigan LCQ DECA XP MAX (Finnigan Corp., San Jose, CA) quadrupole ion trap equipped with an atmospheric pressure ionization (API) source, using an electrospray ionization (ESI) interface. The vaporizer and capillary voltages were 5 kV and 4 V, respectively. The capillary temperature was set at 325 °C. Nitrogen was used as both a sheath and auxiliary gas at flow rates of 90 and 25, respectively (in arbitrary units). Spectra were recorded in positive-ion mode between m/z 250 and 1500. The mass spectrometer was programmed to perform a series of three scans: a full mass, a zoom scan of the most intense ion in the first scan, and a MS−MS of the most intense ion using relative collision energy of 30 and 60 V.

NMR Analysis. ^{1}H NMR (500.13 MHz) and ^{13}C NMR (125.77 MHz) spectra were recorded in CD_3OD on a Bruker-Avance 500 spectrometer at 303 K and with tetramethylsilane (TMS) as an internal standard [chemical shifts (δ) in parts per million and coupling constants (J) in hertz]. Multiplicities are recorded as singlets (s), doublets (d), triplets (t), doublets of doublets (dd), multiplets (m) and unresolved (∗). ^{1}H chemical shifts were assigned using 2D NMR [correlation spectroscopy (COSY)] experiment, while ^{13}C resonances were assigned using 2D NMR techniques (*g*HMBC and *g*HSQC) (*30*, *31*). The delay for the long-range C/H coupling constant was optimized to 7 Hz.

Minimization and Molecular Dynamics. The initial geometries of both isomers, (9*S*,11*R*)- and (9*R*,11*S*)-vinylcatechin dimers, were built with the GaussView (*32*) software. To calculate the optimized geometries and electronic properties, to be used later in the parametrization of these compounds, we used the Gaussian03 suite of programs (*33*) and performed restricted Hartree−Fock (RHF) calculations, with the 6-31G(d) basis set. The atomic charges were further recalculated using RESP (*34*). This methodology was chosen to be consistent with that adopted for the parametrization process in Amber8 software (*35*). Molecular dynamics (MD) simulations were performed for each isomer, with the parametrization adopted in Amber using GAFF, the general force field for small organic molecules. In these simulations, an explicit solvation model with pre-equilibrated TIP3P water molecules was used, filling a truncated octahedral box, with a minimum 12 Å distance between the box faces and any atom of the compound. Each structure was minimized in two stages. In the first stage, the isomers were kept fixed and only the position of the water molecules was minimized. In the second stage, the full system was minimized. Subsequently, a 100 ps equilibration followed by a 10 ns production MD simulations were carried out for each isomer, starting with its optimized structure. The Langevin temperature equilibration scheme (*36*) was used as well as constant volume and periodic boundary conditions. All MD simulations were carried out using the Sander module, implemented in the Amber8 simulations package, with the Cornell force field (*37*). Bond lengths involving hydrogens were constrained using the SHAKE algorithm (*38*), and the equations of motion were integrated with a 2 fs time step using the Verlet leapfrog algorithm. The nonbonded interactions were truncated with a 12 Å cutoff. The temperature of the systems was regulated to be maintained at 303.15 K (*36*).

Conformational Analysis. To study the different conformations obtained for each isomer, the values of the three most important dihedrals in each molecule during all MD simulations were evaluated. All conformations obtained with all combinations of those three dihedrals were considered. Clusters of solutions with similar values of dihedrals for each isomer were obtained. In the end, four and five different conformations for isomers 1 and 2 were obtained, respectively.

The energies of the minimized geometries were calculated for all conformations *in vacuo* with the density functional theory approach, at the unrestricted B3LYP (*39*) hybrid density functional level (Becke−Slater−HF exchange with Lee−Yang−Parr correlation functional) using the 6-31G(d) basis set as implemented in the Gaussian 03 package (*33*). The optimized structures were confirmed as true minima by vibrational analysis performed at the same level of calculation. A scaling factor of 0.9804 and a temperature of 298.150 K were used for vibrational frequency and thermal energy correction calculations.

To evaluate the effect of the aqueous environment, the optimized geometries using a dielectric constant of $\varepsilon = 78.39$ to mimic the water solution were recalculated. Solvation energies were computed with polarizable continuum method (PCM) using the a polarizable conductor calculation model (*40*). Gas-phase corrections were employed to calculate the enthalpy values in the aqueous phase because the calculation of vibrational frequencies with PCM is not very accurate and thermal corrections are expected to be rather similar in both gas and solvated phases.

Upon identification of the optimized geometries for all conformations for both isomers, the larger 6-311+G(2d,2p) basis set was applied to calculate the energy values of all conformers.

RESULTS AND DISCUSSION

Study of the Stability of 8-Vinylcatechin Dimers. The initial time revealed the chromatographic peaks of 8-vinylcatechin and (+)-catechin (panel I in **Figure 1**). After 1 h of reaction, the intensity of the 8-vinylcatechin signal of the solution at pH 3.5 has significantly decreased and four new chromatographic peaks (A, B, C, and D) were detected (panel II in **Figure 1**). After 24 h of reaction, 8-vinylcatechin was not detected (panel III in **Figure 1**).

A similar reaction was performed at pH 2.5 and 4.5 with identical results (**Figure 1**). The decrease of the 8-vinylcatechin concentration was faster with increasing solution acidity.

It was also observed through the peak areas that the formation of peaks A and B is favored at high pH in opposition to the formation of vinylcatechin dimers (peaks C and D), which is favored in more acidic solutions. The peak area of (+)-catechin remained more or less stable, which means that vinylcatechin does not react with the former, undergoing preferentially dimerization reactions.

The reaction mixture was then analyzed by liquid chromatography (LC)−DAD/MS in positive-ion mode. Peak A had the same molecular weight and identical MS data as 8-vinylcatechin. Thus, peak A showed the pseudo-molecular ion $[M + H]^+$ at m/z

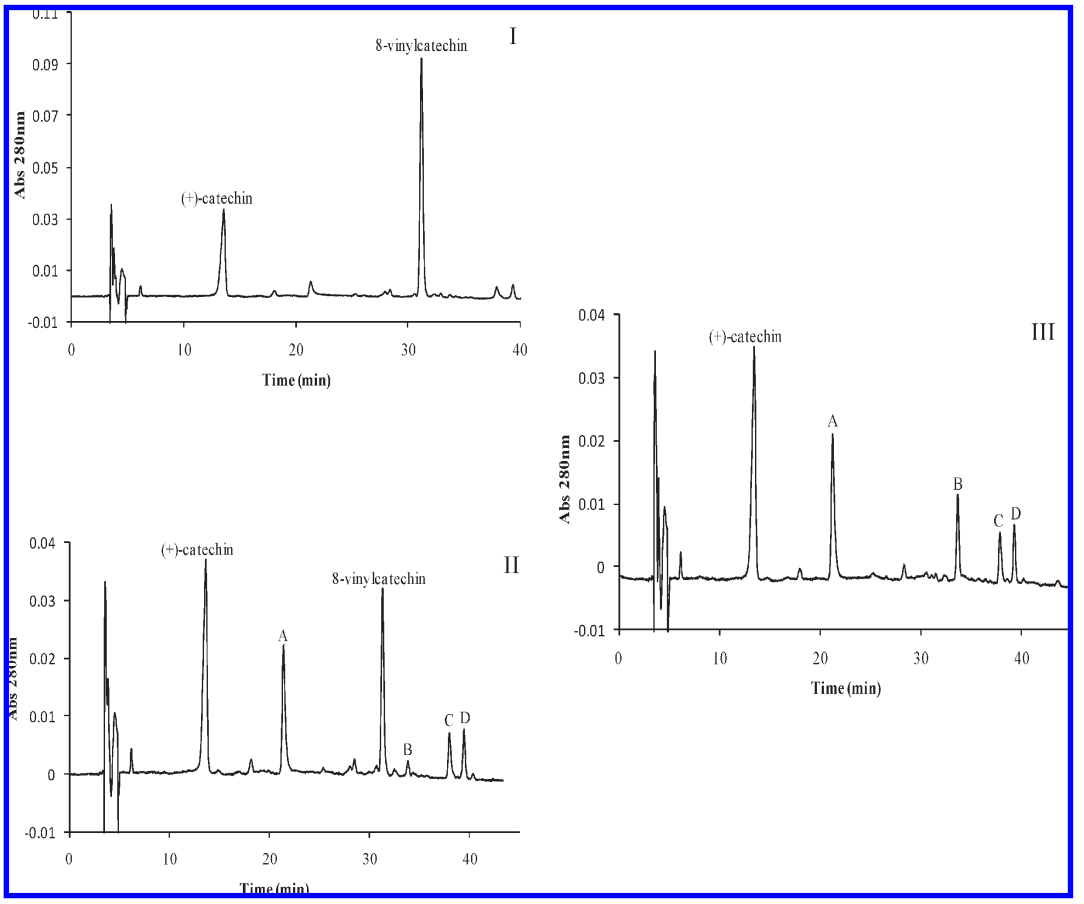

Figure 1. HPLC chromatograms recorded at 280 nm of the hydroalcoholic solution of 8-vinylcatechin at pH 3.5 (I) at the initial time, (II) after 1 h, and (III) after 24 h. Peak A: Dihydrofuran-(+)-catechin, Peak B: 8-ethyl-(+)-catechin and Peaks C and D: Vinylcatechin dimers.

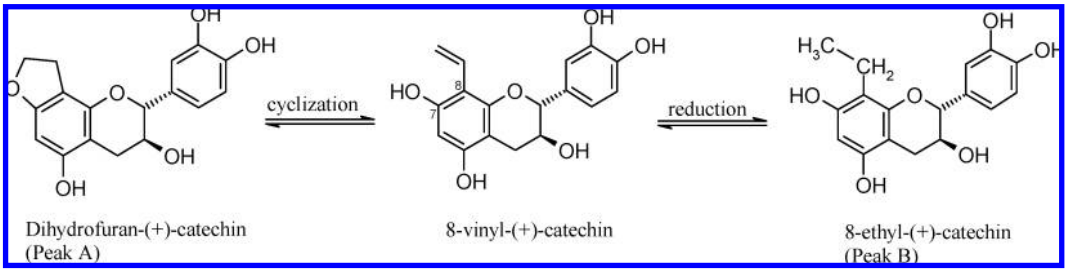

Figure 2. Structures of the compounds corresponding to the chromatographic peaks A and B.

317, a fragment ion $[M + H - 152]^+$ at m/z 165 corresponding to a retro Diels−Alder (RDA) fission of the (+)-catechin moiety, and a fragment ion $[M + H - 152 - 18]^+$ at m/z 147 resulting from a further loss of water. This compound could result from the intramolecular cyclization of the 7-OH group and the vinyl group to give a new dihydrofuran ring (**Figure 2**), which formation is expected to be favored in acid media as previously described with the reaction between malvidin-3-glucoside and 8-vinylcatechin (*27*). Peak B has revealed the pseudo-molecular ion $[M + H]^+$ at m/z 319, which is consistent with the structure of a 8-ethylcatechin. The first fragment ion at $[M + H - 28]^+$ at m/z 291 corresponds to the loss of an ethyl bond, whereas the fragment ion $[M + H - 152]^+$ at m/z 167 corresponds to a RDA fission of the (+)-catechin moiety. This compound could result from the reduction of the vinyl group, giving rise to the ethyl bond (**Figure 2**). Peaks C and D revealed the same pseudo-molecular ion $[M + H]^+$ at m/z 633 and pattern fragmentations that are consistent with the structure of a 8-vinylcatechin dimer. The MS^2 mass spectra showed the fragment ions $[M + H - 316]^+$ at m/z 317 corresponding to the loss of one vinylcatechin unit, $[M + H - 290]^+$ at m/z 343 corresponding to the loss of one (+)-catechin moiety, and $[M + H - 152]^+$ at m/z 481 corresponding to a RDA fission of the (+)-catechin moiety. The MS^3 fragment ion $[M + H - 316 - 152]^+$ at m/z 165 results from a RDA fission of the other (+)-catechin moiety (**Figure 3**).

Synthesis and Isolation of Vinylcatechin Dimers. To increase the formation of vinylcatechin dimers in solution for further isolation and structural characterization, the experimental conditions were developed. 8-Vinylcatechin [containing (+)-catechin as an impurity] was placed in a 20% $EtOH/H_2O$ (pH 2.0) solution. After 2 h, the peak corresponding to 8-vinylcatechin had already disappeared and the isomers 1 and 2 corresponding to the vinylcatechin dimers were detected (**Figure 4**). The formation of vinylcatechin trimers was also detected and further confirmed by MS analysis ($[M + H]^+$ at m/z 949). The reaction mixture was then purified by low-pressure column chromatography (Toyopearl

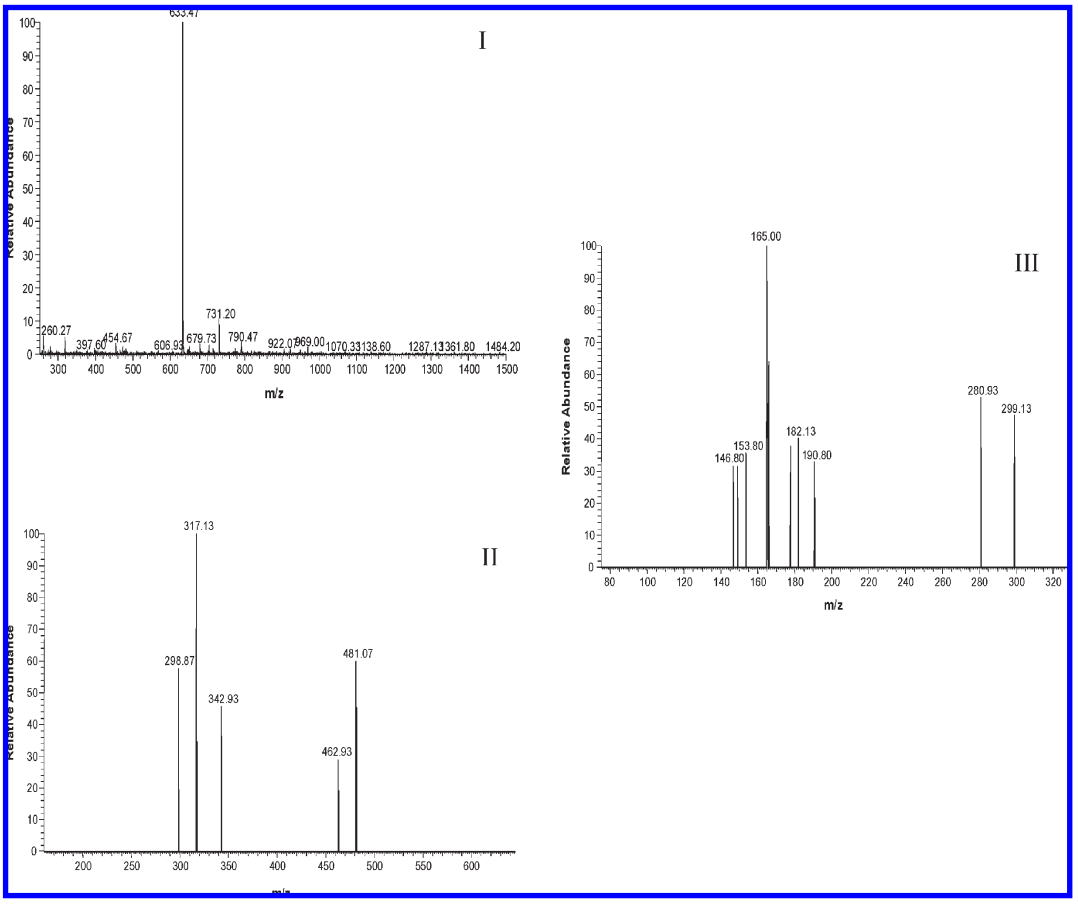

Figure 3. (I) Full MS, (II) MS^2, and (III) MS^3 spectra of 8-vinylcatechin dimers.

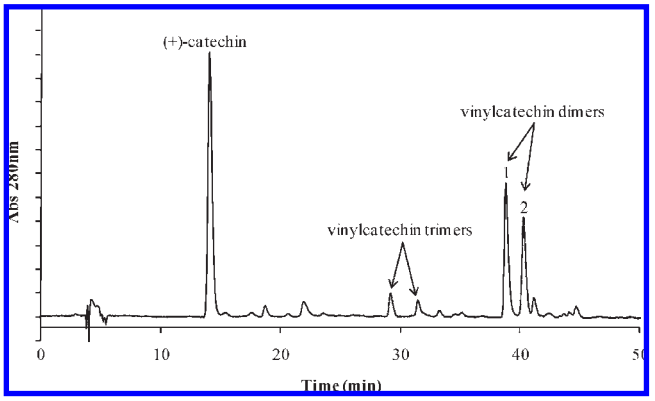

Figure 4. HPLC chromatogram recorded at 280 nm after 2 h of the solution of 8-vinylcatechin at pH 2 containing (+)-catechin as an impurity.

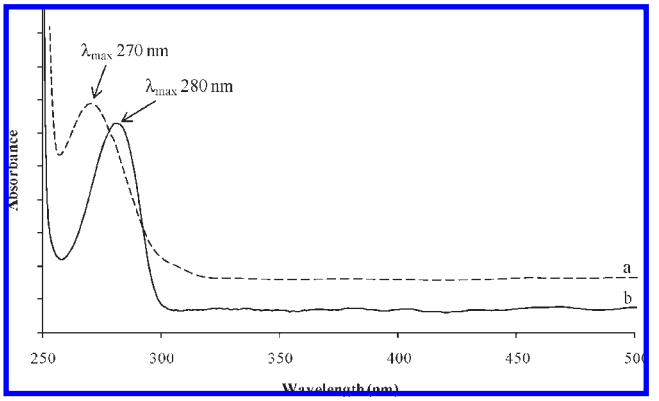

Figure 5. UV−vis spectra recorded from the HPLC−DAD: (a) 8-vinylcatechin and (b) vinylcatechin dimers.

gel), and the vinylcatechin dimers and trimers were isolated. The structures of vinylcatechin dimers were confirmed by NMR, whereas the elucidation of vinylcatechin trimer structures was not possible because of the small amounts of product obtained.

UV−vis spectrum of 8-vinylcatechin dimers revealed an absorbance at λ_{max} of 280 nm, instead of 270 nm, characteristic of 8-vinylcatechin (*29*) (**Figure 5**).

Structural Elucidation of Vinylcatechin Dimers by NMR. The proton and carbon chemical shifts of the vinylcatechin dimers in CD_3OD/TFA (98:2) are shown in **Table 1**.

The proton and carbon chemical shifts of the two isomers were attributed using 1D and 2D NMR techniques [COSY, nuclear Overhauser effect spectrometry (NOESY), heteronuclear single-quantum coherence (HSQC), and heteronuclear multiple-bond correlation (HMBC)].

The protons of the new pyran D ring were attributed through the characteristic ABMX spin system observed in the COSY spectrum. The protons H-10*b*D of isomer 1 and H-10*a*D of isomer 2 were attributed to the triplet of doublets at 2.28 and 2.18 ppm, respectively, presenting a correlation with H-9D (J = 5.6 Hz) and strong correlations with H-11D and H-10*a*,*b*D with the coupling constants J = 11.8 and 13.7 Hz, respectively. The protons H-10*a*D of isomer 1 and H-10*b*D of isomer 2 were determined at 1.60 and 1.65 ppm, respectively, also as a triplet of doublets showing a very small and unresolved coupling constant with proton H-9D and well-defined correlations with protons H-11D and H-10*b*,*a*D (J = 1.5 and 13.7 Hz). The proton

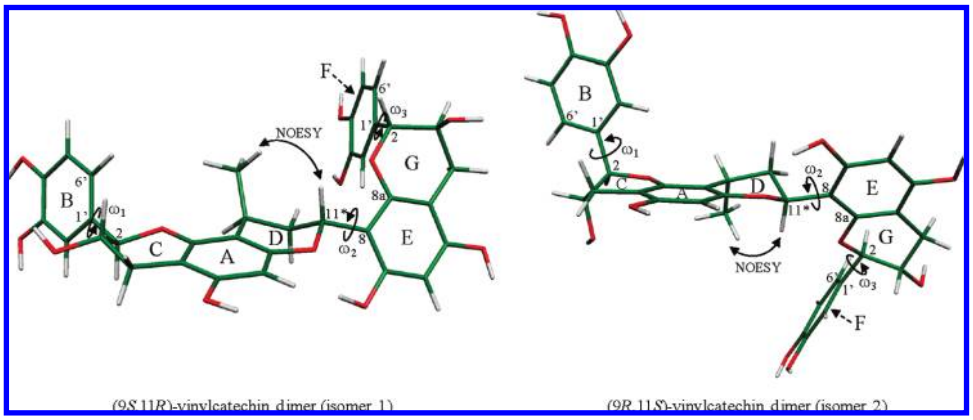

Figure 6. Optimized geometry of conformer 1 obtained for (9*S*,11*R*) and (9*R*,11*S*) isomers.

Table 1. ^{1}H and ^{13}C NMR Data of Vinylcatechin Dimers in CD_3OD/TFA (98:2)[a]

	vinylcatechin dimer (isomer 1)		vinylcatechin dimer (isomer 2)	
position	δ (^{1}H); *J* (Hz)	δ (^{13}C)	δ (^{1}H); *J* (Hz)	δ (^{13}C)
2C	4.66; d, 7.2	81.1	4.65; d, 7.2	81.6
3C	3.99; m	67.2	3.98; m	67.2
4αC	2.87; dd, 5.4/16.2	27.1	2.87; dd, 5.4/16.2	27.1
4βC	2.55; dd, 7.6/16.2		2.55; dd, 7.6/16.2	
2G	4.58; d, 7.6	81.1	4.57; d, 7.6	81.6
3G	3.92; m	67.2	3.91; m	67.2
4αG	2.83; dd, 5.4/16.2	27.1	2.83; dd, 5.4/16.2	27.1
4βG	2.53; dd, 7.6/16.2		2.53; dd, 7.6/16.2	
4aA		99.6		99.8
5A		153.8		153.8
6A	5.99; s	95.5	5.98; s	94.9
7A		154.9		154.9
8A		106.8		106.8
8aA		152.8		152.8
4aE		100.8		101.0
5E		153.8		153.8
6E	5.96; s	95.5	5.97; s	94.9
7E		154.9		154.9
8E		104.3		104.3
8aE		152.4		152.4
1′B		118.5		118.5
2′B	6.9−6.8; ∗	113.5	6.9−6.8; ∗	113.5
3′B		131.0		131.0
4′B		144.8		144.8
5′B	6.8−6.7; ∗	114.6	6.8−6.7; ∗	114.6
6′B	6.7−6.6; ∗	118.3	6.7−6.6; ∗	118.3
1′F		118.5		118.5
2′F	6.9−6.8; ∗	113.5	6.9−6.8; ∗	113.5
3′F		131.0		131.0
4′F		144.8		144.8
5′F	6.8−6.7; ∗	114.6	6.8−6.7; ∗	114.6
6′F	6.7−6.6; ∗	118.3	6.7−6.6; ∗	118.3
9D	2.90; m	24.4	2.86; m	24.4
10*a*D	1.60; td, ∗/1.5/13.7	33.7	2.18; td, 5.6/11.8/13.7	33.9
10*b*D	2.28; td, 5.6/11.8/13.7		1.65; td, ∗/1.5/13.7	
11D	5.48; dd, 1.5/11.8	69.5	5.43; dd, 1.5/11.8	69.5
12	0.97; d, 6.8	20.6	1.07; d, 6.8	20.3

[a] ∗, unresolved; s, singlet; m, multiplet; d, doublet; dd, doublet of doublets; td, triplet of doublets.

H-9D of the isomers 1 and 2 was assigned to the multiplet at 2.90 and 2.86 ppm, respectively, from their correlations with protons H-10*a*,*b*D and protons of the methyl group (H-12). The proton H-11D was attributed to the doublet of doublets at 5.48 ppm (isomer 1) and 5.43 ppm (isomer 2) from their weak correlation

Table 2. ΔH Values of Each Conformer for Both Isomers in an Aqueous Environment Are Shown as Well as the Values Obtained for the Dihedrals ω_1, ω_2, and ω_3

isomer	conformation	ΔH (kcal/mol)[a]	ω_1	ω_2	ω_3
(9*S*,11*R*)	1	0.00 (−2217.825433 au)	−54.32	−140.92	−47.04
	2	1.07	122.75	−148.79	−40.16
	3	1.50	−54.78	−145.84	151.34
	4	4.00	−18.98	−138.21	27.74
(9*R*,11*S*)	1	0.00 (−2217.825091 au)	−108.91	−125.83	−72.41
	2	4.04	−49.67	145.14	160.14
	3	2.68	154.22	144.43	−13.69
	4	23.61	159.98	144.10	131.37
	5	3.11	−22.02	144.76	165.78

[a] All calculated ΔH values are related to conformation 1 of each isomer.

with proton H-10*b*D (J = 1.5 Hz) and strong correlation with proton H-10*a*D (J = 11.8 Hz). The protons of methyl group (H-12) were attributed to the doublet at 0.97 ppm (isomer 1) and 1.07 ppm (isomer 2), through the correlation with H-9D (J = 6.8 Hz).

H-9D, H-12, H-10*a*,*b*D, and H-6A also show a ^{1}H−^{13}C correlation (HMBC) with carbon C-8A located at 106.8 ppm, whereas the protons H-11D and H-6E show a long-distance correlation with carbon C-8E (104.3 ppm).

The carbons C-9, C-10, and C-11 of the pyran ring D and C-12 were easily assigned from their direct ^{1}H−^{13}C correlations observed in the HSQC spectrum with respective protons.

The carbons C-8aA and C-8aE were assigned at 152.8 and 152.4 ppm, respectively, from correlations with protons H-4α,βC, G and H-2C,G. Their differentiation was possible through the correlation of C-8aA with H-9D, whereas C-8aE was correlated with proton H-11D.

The two isomers 1 and 2 are diasteroisomers differing in the stereochemistry of the two C-9 and C-11 asymmetric carbons of the newly formed pyran ring D.

The relative configuration of the asymmetric carbons C-9 and C-11 was determined through the NOESY correlation of the methyl group (C-12) and H-11D. In both isomers, protons of the methyl group showed correlations with proton H-11D, which means that they are close in the same side of the molecular plan: in one isomer, both protons of the methyl group and H-11D are oriented upward in the plan (9*S*,11*R* or 9*R*,11*S*), and in the other isomer, they are oriented downward in the plan (9*R*,11*S* or 9*S*,11*R*) (**Figure 5**). To attribute the correct relative configuration of isomers 1 and 2, stability studies of (9*S*,11*R*)- and (9*R*,11*S*)-vinylcatechin dimers using theoretical and computational methods were performed. On the basis of the ^{1}H NMR intensity, the

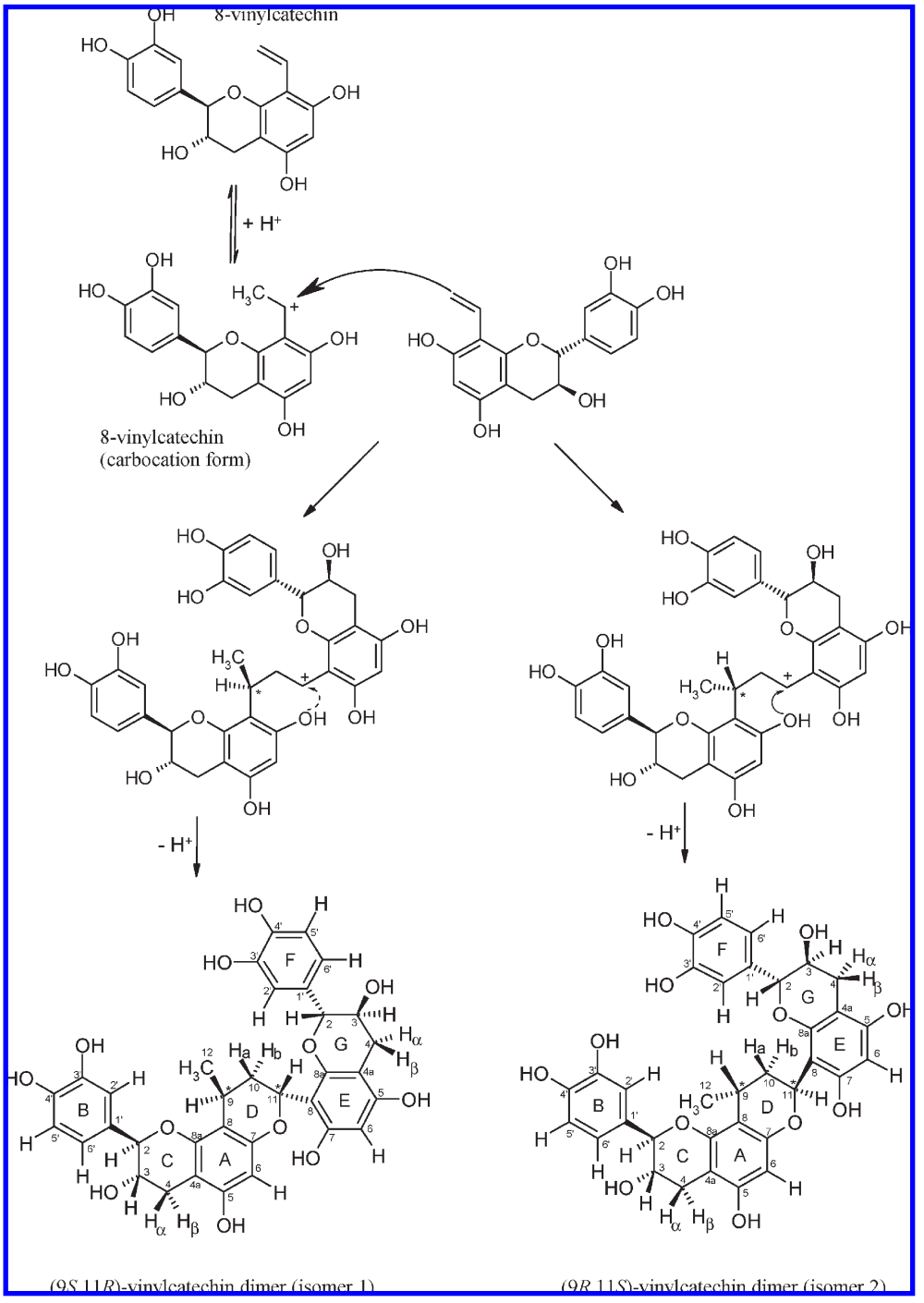

Figure 7. Proposed formation mechanism of the vinylcatechin dimers ($[M + H]^+$ at *m/z* 633) in acidic medium.

isomer 1/isomer 2 molar ratio was 1:0.9, which means that isomer 1 should be slightly more stable than isomer 2 (lower energy level).

Theoretical and Computational Studies. The MD simulations performed for each isomer allowed sampling of their respective conformational space and, therefore, to identify their different conformations. To study the latter, the values of the most crucial dihedrals responsible for the conformational variations during each MD simulation were analyzed. These dihedrals were ω_1 (C6′−C1′−C2−O), ω_2 (O−C11*−C8−C8a), and ω_3 (O−C2−C1−C6′). When all of the arrangements obtained with the different values of the dihedrals ω_1, ω_2, and ω_3 were combined, all structures obtained were clustered and, in the end, isomers (9*S*,11*R*) and (9*R*,11*S*) did show four and five different conformations, respectively. Subsequently, all structures were optimized in vacuum as well as in an aqueous environment. To compare the solvated energies of both isomers, a larger 6-311+G(2d,2p) basis set was tested with single-point calculations in all optimized solvated geometries. **Table 2** displays the change in enthalpy ($\triangle H$) values of all conformations relative to the most stable conformation for each isomer in aqueous solution with this larger basis sets and after the addition of thermal corrections. The values of the dihedrals ω_1, ω_2, and ω_3 are also shown.

The energy values obtained for all conformational structures for each isomer are very similar in both cases. Isomer (9*S*,11*R*) displays a difference of 4.00 kcal/mol between the most and least thermodynamically favorable conformations, while in isomer (9*R*,11*S*), this difference increases to 23.61 kcal/mol.

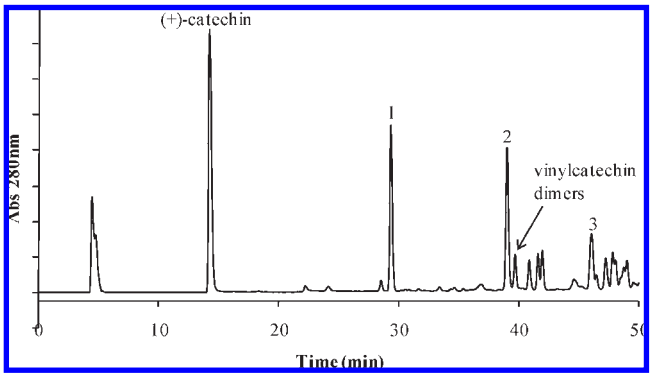

Figure 8. HPLC chromatogram recorded at 280 nm of the reaction between (+)-catechin and acetaldehyde at pH 4. The other isomer is possibly masked by peak 2. Peaks 1, 2, and 3: 8,8-methylmethine catechin-catechin isomers.

Furthermore, comparing the values obtained for the most favorable conformation of each isomer (both conformer number 1), the difference in their energies is 0.21 kcal/mol. Therefore, the results show that isomer (9*S*,11*R*) possesses higher stability and its formation is thermodynamically favored when compared to isomer (9*R*,11*S*). According to the Maxwell−Boltzmann distribution (using the temperature of 303.15 K), this small difference is in agreement with the experimental NMR results obtained in this work [55% of the isomer (9*S*,11*R*) and 45% of isomer (9*R*,11*S*)].

Analyzing the optimized geometries in vacuum and in aqueous solution, it was found that the structures are very similar to each other. According to the geometries obtained for all conformations, a short hydrogen interaction (approximately 1.80 Å) established between the oxygen of the D ring and the hydroxyl group of C7 of the E ring was observed. Our results demonstrate that the equatorial position of the vinylcatechin group substituent bound to the C7* chiral center is important for the establishment of this important bridge. The only exception occurs in conformation 4 of isomer (9*R*,11*S*), in which the vinylcatechin group adopts an axial position, which precludes the formation of the hydrogen bond.

Figure 6 shows the optimized continuum geometries, for the most thermodynamically favored conformer for both isomers. The optimized geometry adopted by the majority of the conformations for both isomers reveals that the most favorable conformers have the vinylcatechin groups facing opposite sides.

Mechanism of Formation. The formation of vinylcatechin dimers should result from an unusual acid-catalyzed dimerization of vinyl compounds through a mechanism involving the formation of a new dihydropyran ring D (**Figure 7**). In acid medium, one 8-vinylcatechin molecule is rapidly protonated, giving a carbocation that then undergoes a nucleophilic attack from a vinyl group of the other 8-vinylcatechin molecule, yielding two carbocations differing in the stereochemistry of C-9. Further intramolecular nucleophilic attack of the hydroxyl group from ring A to the positively charged C-11 (intramolecular cyclization) leads to the formation of a new pyranic ring D. The stereochemistry of C-11 also differs from the side of the OH nucleophilic attack.

Reactions between (+)-Catechin and Acetaldehyde. Reactions between (+)-catechin and acetaldehyde at different pH values (3, 4, and 6) were carried out to detect the formation of vinylcatechin dimers. The reaction mixtures were analyzed by LC−DAD/MS in positive-ion mode. The chromatographic peaks 1, 2, and 3 corresponding to the 8,8-methylmethine catechin−catechin isomers ($[M + H]^+$ at m/z 607) as well as the minor peaks corresponding to the 8,8-methylmethine catechin−catechin−catechin isomers ($[M + H]^+$ at m/z 923) were detected in all solutions, as already reported (*41*). The formation of the isomers of vinylcatechin dimers, although in small quantities, was found to be higher in the reaction at pH 4. The presence of these compounds was confirmed by their mass spectra and retention times, which are identical to the ones described above for 8-vinylcatechin dimerization (**Figure 8**).

In conclusion, 8-vinylcatechin revealed to be a very unstable molecule in acidic model solutions undergoing rapid transformations giving rise to several vinylcatechin derivatives, which explains in part why its presence has never been detected in wines or in model wine solutions. Two of these compounds correspond to diasteroisomers of vinylcatechin dimers, and their structures were described herein for the first time. This kind of compound was also found to occur in model solutions resulting from reactions of (+)-catechin with acetaldehyde. 8-vinylcatechin also showed great reactivity with (+)-catechin, yielding a 8,8-methylmethine catechin−catechin already reported in reactions between (+)-catechin and acetaldehyde. These preliminary results bring new important information about the behavior of 8-vinylcatechin in solution. In fact, because of its already demonstrated extreme reactivity with anthocyanins and possibly with other compounds present in wines, 8-vinylcatechin could certainly have a significant contribution to the phenolic composition of aged wines.

LITERATURE CITED

(1) Beecher, G. R. Overview of dietary flavonoids: Nomenclature, occurrence and intake. *J. Nutr.* **2003**, *133*, 3248S–3254S.
(2) Manach, C.; Scalbert, A.; Morand, C.; Remesy, C.; Jimenez, L. Polyphenols: Food sources and bioavailability. *Am. J. Clin. Nutr.* **2004**, *79*, 727–747.
(3) Fulcrand, H.; Atanasova, V.; Salas, E.; Cheynier, V. The fate of anthocyanins in wine: Are there determining factors? In *Red Wine Color: Revealing the Mysteries*; Waterhouse, A. L., Kennedy, J. A., Eds.; Oxford University Press: New York, 2004; pp 68−88.
(4) de Freitas, V.; Mateus, N. Chemical transformations of anthocyanins yielding a variety of colours (Review). *Environ. Chem. Lett.* **2006**, *4*, 175–183.
(5) Es-Safi, N. E.; Ghidouche, S.; Ducrot, P. H. Flavonoids: Hemisynthesis, reactivity, characterization and free radical scavenging activity. *Molecules* **2007**, *12*, 2228–2258.
(6) Somers, T. C. The polymeric nature of wine pigments. *Phytochemistry* **1971**, *10*, 2175–2186.
(7) Remy, S.; Fulcrand, H.; Labarbe, B.; Cheynier, V.; Moutounet, M. First confirmation in red wine of products resulting from direct anthocyanin−tannin reactions. *J. Sci. Food Agric.* **2000**, *80*, 745–751.
(8) Timberlake, C. F.; Bridle, P. Interactions between anthocyanins, phenolic compounds and acetaldehyde and their significance in red wines. *Am. J. Enol. Vitic.* **1976**, *27*, 97–105.
(9) Rivas-Gonzalo, J. C.; Bravo-Haro, S.; Santos-Buelga, C. Detection of compounds formed through the reaction of malvidin-3-monoglucoside and catechin in the presence of acetaldehyde. *J. Agric. Food Chem.* **1995**, *43*, 1444–1449.
(10) Pissarra, J.; Lourenco, S.; Gonzalez-Paramas, A. M.; Mateus, N.; Santos-Buelga, C.; de Freitas, V. Formation of new anthocyanin-alkyl/aryl-flavanol pigments in model solutions. *Anal. Chim. Acta* **2004**, *513*, 215–221.
(11) Rentzsch, W.; Schwarz, M.; Winterhalter, P. Pyranoanthocyanins—An overview on structures, occurrence, and pathways of formation. *Trends Food Sci. Technol.* **2007**, *18*, 526–534.
(12) Bakker, J.; Timberlake, C. F. Isolation, identification, and characterization of new color-stable anthocyanins occurring in some red wines. *J. Agric. Food Chem.* **1997**, *45*, 35–43.
(13) Fulcrand, H.; Benabdeljalil, C.; Rigaud, J.; Cheynier, V.; Moutounet, M. A new class of wine pigments generated by reaction between pyruvic acid and grape anthocyanins. *Phytochemistry* **1998**, *47*, 1401–1407.

(14) Mateus, N.; Silva, A. M. S.; Vercauteren, J.; de Freitas, V. Occurrence of anthocyanin-derived pigments in red wines. *J. Agric. Food Chem.* **2001**, *49*, 4836–4840.
(15) Bakker, J.; Bridle, P.; Honda, T.; Kuwano, H.; Saito, N.; Terahara, N.; Timberlake, C. F. Isolation and identification of a new anthocyanin occurring in some red wines. *Phytochemistry* **1997**, *44*, 1375–1382.
(16) Francia-Aricha, E. M.; Guerra, M. T.; Rivas-Gonzalo, J. C.; Santos-Buelga, C. New anthocyanin pigments formed after condensation with flavanols. *J. Agric. Food Chem.* **1997**, *45*, 2262–2265.
(17) Mateus, N.; Carvalho, E.; Carvalho, A. R. F.; Melo, A.; Gonzalez-Paramas, A. M.; Santos-Buelga, C.; Silva, A. M. S.; de Freitas, V. Isolation and structural characterization of new acylated anthocyanin−vinyl−flavanol pigments occurring in aging red wines. *J. Agric. Food Chem.* **2003**, *51*, 277–282.
(18) Mateus, N.; de Pascual-Teresa, S.; Rivas-Gonzalo, J. C.; Santos-Buelga, C.; de Freitas, V. Structural diversity of anthocyanin-derived pigments in port wines. *Food Chem.* **2002**, *76*, 335–342.
(19) Mateus, N.; Silva, A. M. S.; Santos-Buelga, C.; Rivas-Gonzalo, J. C.; de Freitas, V. Identification of anthocyanin−flavanol pigments in red wines by NMR and mass spectrometry. *J. Agric. Food Chem.* **2002**, *50*, 2110–2116.
(20) Mateus, N.; Oliveira, J.; Gonzalez-Paramas, A. M.; Santos-Buelga, C.; de Freitas, V. Screening of portisins (vinylpyranoanthocyanin pigments) in port wine by LC/DAD−MS. *Food Sci. Technol. Int.* **2005**, *11*, 353–358.
(21) Mateus, N.; Oliveira, J.; Haettich-Motta, M.; de Freitas, V. New family of bluish pyranoanthocyanins. *J. Biomed. Biotechnol.* **2004**, 299–305.
(22) Mateus, N.; Oliveira, J.; Pissarra, J.; Gonzalez-Paramas, A. M.; Rivas-Gonzalo, J. C.; Santos-Buelga, C.; Silva, A. M. S.; de Freitas, V. A new vinylpyranoanthocyanin pigment occurring in aged red wine. *Food Chem.* **2006**, *97*, 689–695.
(23) Mateus, N.; Oliveira, J.; Santos-Buelga, C.; Silva, A. M. S.; de Freitas, V. NMR structure characterization of a new vinylpyranoanthocyanin−catechin pigment (a portisin). *Tetrahedron Lett.* **2004**, *45*, 3455–3457.
(24) Mateus, N.; Silva, A. M. S.; Rivas-Gonzalo, J. C.; Santos-Buelga, C.; de Freitas, V. A new class of blue anthocyanin-derived pigments isolated from red wines. *J. Agric. Food Chem.* **2003**, *51*, 1919–1923.
(25) Oliveira, J.; de Freitas, V.; Silva, A. M. S.; Mateus, N. Reaction between hydroxycinnamic acids and anthocyanin−pyruvic acid adducts yielding new portisins. *J. Agric. Food Chem.* **2007**, *55*, 6349–6356.
(26) Oliveira, J.; Santos-Buelga, C.; Silva, A. M. S.; de Freitas, V.; Mateus, N. Chromatic and structural features of blue anthocyanin-derived pigments present in Port wine. *Anal. Chim. Acta* **2006**, *563*, 2–9.
(27) Cruz, L.; Teixeira, N.; Silva, A. M. S.; Mateus, N.; Borges, J.; de Freitas, V. Role of vinylcatechin in the formation of pyranomalvidin-3-glucoside−(+)-catechin. *J. Agric. Food Chem.* **2008**, *56*, 10980–10987.
(28) Es-Safi, N. E.; Fulcrand, H.; Cheynier, V.; Moutounet, M. Studies on the acetaldehyde-induced condensation of (−)-epicatechin and malvidin 3-*O*-glucoside in a model solution system. *J. Agric. Food Chem.* **1999**, *47*, 2096–2102.
(29) Cruz, L.; Borges, E.; Silva, A. M. S.; Mateus, N.; de Freitas, V. Synthesis of a new (+)-catechin-derived compound: 8-Vinylcatechin. *Lett. Org. Chem.* **2008**, *5*, 530–536.
(30) Bax, A.; Subramanian, S. Sensitivity enhanced two-dimensional heteronuclear shift correlation NMR spectroscopy. *J. Magn. Reson.* **1986**, *67*, 565–569.
(31) Bax, A.; Summers, M. F. ^{1}H and ^{13}C assignments from sensitivity-enhanced detection of heteronuclear multiple-bond connectivity by 2D multiple quantum NMR. *J. Am. Chem. Soc.* **1986**, *108*, 2093–2094.
(32) Gaussian Inc., Carnegie Office Park, Building 6, Pittsburgh, PA 15106.
(33) Frisch, M. J.; Trucks, G. W.; Schlegel, H. B.; Scuseria, G. E.; Robb, M. A.; Cheeseman, J. R.; Montgomery, J. A., Jr.; Vreven, T.; Kudin, K. N.; Burant, J. C.; Millam, J. M.; Iyengar, S. S.; Tomasi, J.; Barone, V.; Mennucci, B.; Cossi, M.; Scalmani, G.; Rega, N.; Petersson, G. A.; Nakatsuji, H.; Hada, M.; Ehara, M.; Toyota, K.; Fukuda, R.; Hasegawa, J.; Ishida, M.; Nakajima, T.; Honda, Y.; Kitao, O.; Nakai, H.; Klene, M.; Li, X.; Knox, J. E.; Hratchian, H. P.; Cross, J. B.; Bakken, V.; Adamo, C.; Jaramillo, J.; Gomperts, R.; Stratmann, R. E.; Yazyev, O.; Austin, A. J.; Cammi, R.; Pomelli, C.; Ochterski, J. W.; Ayala, P. Y.; Morokuma, K.; Voth, G. A.; Salvador, P.; Dannenberg, J. J.; Zakrzewski, V. G.; Dapprich, S.; Daniels, A. D.; Strain, M. C.; Farkas, O.; Malick, D. K.; Rabuck, A. D.; Raghavachari, K.; Foresman, J. B.; Ortiz, J. V.; Cui, Q.; Baboul, A. G.; Clifford, S.; Cioslowski, J.; Stefanov, B. B.; Liu, G.; Liashenko, A.; Piskorz, P.; Komaromi, I.; Martin, R. L.; Fox, D. J.; Keith, T.; Al-Laham, M. A.; Peng, C. Y.; Nanayakkara, A.; Challacombe, M.; Gill, P. M. W.; Johnson, B.; Chen, W.; Wong, M. W.; Gonzalez, C.; Pople, J. A. Gaussian 03, Inc., revision B.04 ed.; Pittsburgh, PA, **2003**.
(34) Bayly, C. I.; Cieplak, P.; Cornell, W. D.; Kollman, P. A. A well-behaved electrostatic potential based method using charge restraints for deriving atomic charges: The RESP model. *J. Phys. Chem.* **1993**, *97*, 10269–10280.
(35) Case, D. A.; Darden, T. A.; Cheatham, T. E., III; Simmerling, C. L.; Wang, J.; Duke, R. E.; Luo, R.; Merz, H. M.; Wang, B.; Pearlman, D. A.; Crowley, M.; Brozell, S.; Tsui, V.; Gohlke, H.; Mongan, J.; Hornak, V.; Cui, G.; Beroza, P.; Schafmeister, C.; Caldwell, J. W.; Ross, W. S.; Kollman, P. A. AMBER 8; University of California, San Francisco, CA, **2004**.
(36) Izaguirre, J. A.; Catarello, D. P.; Wozniak, J. M.; Skeel, R. D. Langevin stabilization of molecular dynamics. *J. Chem. Phys.* **2001**, *114*, 2090–2098.
(37) Cornell, W. D.; Cieplak, P.; Bayly, C. I.; Gould, I. R.; Merz, K. M.; Ferguson, D. M.; Spellmeyer, D. C.; Fox, T.; Caldwell, J. W.; Kollman, P. A. A 2nd generation force-field for the simulation of proteins, nucleic acids, and organic molecules. *J. Am. Chem. Soc.* **1995**, *117*, 5179–5197.
(38) Ryckaert, J. P.; Ciccotti, G.; Berendsen, H. J. C. Numerical-integration of Cartesian equations of motion of a system with constraints—Molecular-dynamics of *n*-alkanes. *J. Comput. Phys.* **1977**, *23*, 327–341.
(39) Becke, A. D. Density-functional thermochemistry. 4. A new dynamical correlation functional and implications for exact-exchange mixing. *J. Chem. Phys.* **1996**, *104*, 1040–1046.
(40) Tomasi, J.; Mennucci, B.; Cammi, R. Quantum mechanical continuum solvation models. *Chem. Rev.* **2005**, *105*, 2999–3093.
(41) Fulcrand, H.; Doco, T.; Es-Safi, N.-E.; Cheynier, V.; Moutounet, M. Study of the acetaldehyde induced polymerisation of flavan-3-ols by liquid chromatography−ion spray mass spectrometry. *J. Chromatogr., A* **1996**, *752*, 85–91.

Received May 14, 2009. Revised manuscript received August 3, 2009. Accepted September 22, 2009. This research was supported by the research project grants (PTDC/QUI/67681/2006) and CONC-REEQ/275/2001 funding from Fundação para a Ciência e a Tecnologia (FCT) from Portugal. Luís Cruz gratefully acknowledges a Ph.D. grant from FCT (SFRH/BD/30915/2006).